Sub-THz Wireless Over Fiber for Frequency Band 220–280 GHz

Haymen Shams, Martyn J. Fice, *Member, IEEE*, Luis Gonzalez-Guerrero, Cyril C. Renaud, *Senior Member, IEEE*, Frédéric van Dijk, and Alwyn J. Seeds, *Fellow, IEEE*

Abstract—Higher capacity wireless access networks are required to serve the growing demands for mobile traffic and multimedia services. The use of sub-THz carrier frequencies is a potential solution for the increased data demands. This paper proposes and demonstrates experimentally the photonic generation of a multi-band signal for sub-THz wireless-over-fiber transmission at up to 100 Gbit/s (20 Gbit/s in each band) using the full spectrum 220–280 GHz for downlink wireless transmission and an uplink with 10 Gbit/s on-off keying. By using an optical frequency comb generator (OFCG), five optical tones spaced by 15 GHz are selected and split into odd and even optical subcarriers modulated separately using 10 Gbaud quadrature phase shift keying with Nyquist bandwidth achieved by using root raised cosine filtering with 0.01 roll off factor. These optical subcarriers are combined and transmitted over 10 km of fiber to the remote antenna unit (RAU). The optical bands are then filtered and transmitted separately at the RAU in a wireless channel. The received sub-THz band is down-converted to the intermediate frequency and digital signal processing (DSP) is employed at the receiver to measure the bit error ratio (BER). The performance is also evaluated to investigate the impact of the uplink on the downlink optical transmission. The receiver link budget and wireless distance for acceptable BER are also explored. The proposed system aims to distribute sub-band THz signals for short range indoor mobile units. The overall transmission capacity is increased by transmitting it as a multiband, which also reduces the bandwidth requirements on opto-electronicdevices.

Index Terms—Digital coherent detection, fiber wireless, high-speed wireless, optical heterodyning, photonic THz generation, radio-over-fiber.

I. INTRODUCTION

ACCORDING to Cisco's visual networking index forecast, it is expected that annual global IP wireless data traffic will exceed 24.3 Exabytes per month by 2019, and will continue to increase [1]. This is mainly driven by the exponential increase in the number of wireless gadgets such as smart phones,
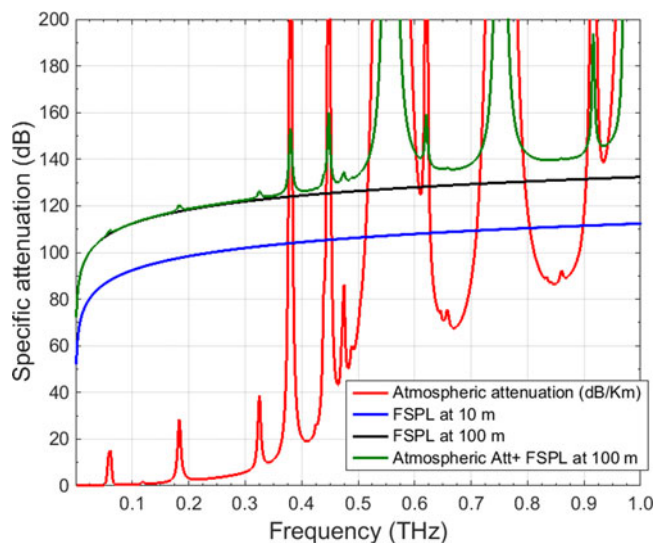

Fig. 1. Specific attenuation due to atmospheric gases based on calculated model ITU-R P676-10 for an air pressure of 1013 hPa, a temperature of 15 °C and a water vapor density of 7.5 g/m [5].

tablets, and video streaming. In addition, the Internet of Things (IoT), where a wide range of miscellaneous devices are connected to the Internet, is expected to grow extremely rapidly from 10.3 million devices in 2014 to more than 29.5 million in 2020 [2]. Therefore, the wireless network will need to support the demand for more network capacity, which is now considered as a motivation for 5G wireless development. This includes the potential move to millimetre-wave (mm-wave) band with a massive bandwidth, and extreme base station and device densities [3], [4].

The fundamental challenges at these mm-waves are high free space path loss (FSPL), and atmospheric absorption due water vapour molecules. Fig. 1 shows the specific attenuation due to atmospheric gases and the absorption peaks over a range of frequencies up to 1 THz using an ITU-R model, and also the FSPL with and without atmospheric attenuation at 10 m and 100 m [5]. Above 100 GHz, there are several frequency windows between water absorption lines, which could be used for indoor short-range systems. The 220–320 GHz frequency band is a large transmission window (100 GHz) without molecular absorption lines. An atmospheric attenuation of 3–8 dB/km is observed under standard earth atmosphere conditions using the ITU-R model [5]. However, it is clear that for these windows the main issue is FSPL (100 m at 200 GHz corresponds to about 120 dB). When combined with limited transmitter power, it is

clear that such a system requires directional and line-of-sight systems instead of the omni-directional antennas used at low GHz radio frequencies. In this case, synergies between fiber-based access networks and THz wireless links enable THz signal distribution over wide areas, while maintaining acceptable wireless power budgets. In addition, all the resources of optical communications and photonic methods can be adapted for THz wireless communications, such as using high spectral efficiency data modulation formats, wavelength division multiplexing technology for multichannel THz wireless links, and coherent optical receivers for impairment compensation using digital signal processing (DSP).

Research in the W-band (75–110 GHz) and higher mm-wave bands has shown much interest in exploiting these bands for broadband wireless communications. At 120 GHz, a wireless link was first demonstrated for single channel transmission of 10 Gbit/s data over 1 km in a real-time system using amplitude shift keying (ASK) [6]. The primary proposed application is mainly to increase the backhaul wireless in the event of hard-to-install fiber networks, or in the case of emergency disaster recovery. Increased bit rate was also investigated in the W-band, by using higher level modulation formats and polarization multiplexing schemes. By using either of the techniques or both, the spectral efficiency of the system increases. However, this required a coherent receiver and off-line DSP to measure the system performance. Transmission of 20 Gbit/s quadrature phase shift keying (QPSK) and 40 Gbit/s 16 quadrature amplitude modulation (16-QAM) were demonstrated with spectral efficiency of 1 bit/s/Hz and 2 bit/s/Hz, respectively and for very small wireless transmission distance [7], [8]. Moreover, using antenna polarization diversity techniques and optical polarization division multiplexing (PDM) 16QAM, the transmission capacity reached up to 100 Gbit/s (with spectral efficiency 4 bits/s/Hz) over a single wide RF-bandwidth in a single channel [9]. Other schemes have also shown demonstration of a full duplex transmission signal with 120 Gbit/s PDM-QPSK (2 bit/s/Hz) and using the wireless link as a bridge between two fiber access networks over physical obstacles [10]. A multiple channels approach was also used to enable transmission for different users with lower data rate signals and to relax the power and bandwidth requirement for electro-optical devices, and digital-to-analog conversions (DAC). A single and four channels at 9.6 Gbit/s per channel were experimentally demonstrated using electrical orthogonal frequency division multiplexing (OFDM) and 16-QAM for 1.3 m wireless distance [11]. Wireless multichannel with total capacity of 120 Gbit/s was also achieved at 92 GHz based on PDM and QPSK [12].

In the 200–300 GHz band, there has also been strong interest due to relatively low atmospheric transmission losses. Data rates of up to 100 Gbit/s were achieved at 237.5 GHz by using different modulation formats for each of three channels and a monolithic millimeter-wave integrated circuit (MMIC) receiver [13]. There have also been several demonstrations of high-data-rate wireless transmission above 300 GHz. 40 Gbit/s ASK (0.5 bit/s/Hz) was achieved at 300 GHz using a direct detection scheme [14]. At 325 GHz signal transmission of 20 Gbit/s
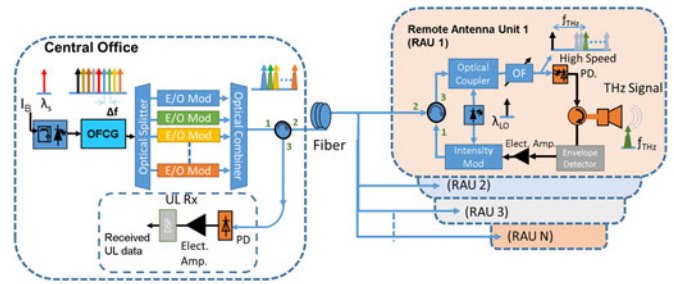

Fig. 2.   Proposed photonic multiband wireless-over-fiber system.

QPSK (2 bit/s/Hz) was also demonstrated over 15 m [15], and 46 Gbit/s was realized at 400 GHz using a THz photomixer integrated with a broadband antenna [16]. Recently, we demonstrated up to 100 Gbit/s multichannel transmission with closely spaced subcarriers at 200 GHz carrier frequency and 2 bit/s/Hz spectral efficiency using two free-running lasers or an externally injected gain switched laser and a digital coherent receiver [17]–[19]. However, this was implemented for a single band to only a single user.

In this paper, we demonstrate experimentally photonic generation of multiband sub-THz wireless-over-fiber signals at up to 100 Gbit/s using the full band from 220–280 GHz for the downlink stream, with spectral efficiency of about 1.33 bit/s/Hz per channel, and 10 Gbit/s on-off keying (OOK) for the uplink stream. We focus here on short-range indoor link distribution, examining the usage of the whole THz bandwidth. No power amplifiers at emission or reception are used in this work. An optical frequency comb generator (OFCG) was employed to generate optical phase correlated tones spaced by 15 GHz. Five optical tones were selected and split into odd and even subcarriers. Then, these optical subcarriers were modulated with uncorrelated 10 Gbaud QPSK with Nyquist bandwidth achieved by using a root raised cosine (RRC) filter with 0.01 roll-off factor, giving a spectral efficiency of 1.33 bit/s/Hz). Single- and multi-band sub-THz wireless signals were demonstrated using heterodyne mixing of the optically modulated 10 Gbaud QPSK signals with a local oscillator (LO) optical source at the remote antenna unit (RAU). The system performance was evaluated by measuring the bit error ratio (BER) for a 10 km fiber link length between the optical transmitter and the RAU. The uplink impact on the downlink channel was also investigated. The receiver link power budget and wireless distance were studied in terms of the received electrical power and BER measurements.

II. Configuration for Multiband Sub-THz Wireless-Over-Fiber System

The arrangement of the multiband sub-THz wireless-over-fiber system for up- and down- links is shown in Fig. 2. For the downlink stream, a single wavelength laser is used to generate optical coherent tones in an OFCG, which is a very convenient way to create a number of phase-correlated optical carriers. These optical carriers are spaced by the driving RF frequency,
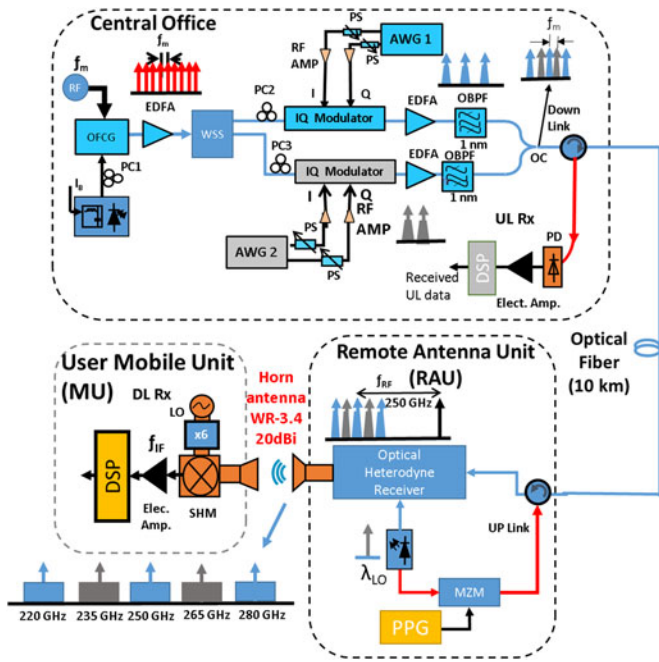
Fig. 3. Schematic diagram for multiband sub-THz wireless-over-fiber experiment.

Fig. 4. Optical spectral for (a) OFCG output, and (b) after filtering odd and even channels.

and then are de-multiplexed and individually modulated. After that, the modulated optical tones are combined and transmitted over a length of standard single mode fiber (SSMF) to different RAUs.

At the RAU, the received optical multiband signal is coupled with an LO light source to generate an optical heterodyne signal. An optical filter or a wavelength selective switch (WSS) is used to select one sub-band and the LO laser, which is launched into a high-speed photodiode (PD) to generate the sub-THz modulated signal. This sub-THz signal is then radiated through an antenna to the user mobile unit. This configuration allows the RAU to be reconfigurable and enables frequency reuse capability by using a tuneable LO laser to adjust the transmit carrier frequency, giving it more flexibility for picocell system architectures. In addition, this system enables the transmitted data rate to be increased while using reduced bandwidth of opto-electronic devices.

For the uplink stream, the received THz signal is envelope detected, and electrically amplified before being used to drive an intensity modulator. The antenna is connected to a microwave circulator for up/down link separation. The LO laser used for upconverting the downlink is also used for the uplink stream. Then, the baseband signal is transmitted over the same fiber to the central office where it is photodetected and demodulated.

III. EXPERIMENTAL ARRANGEMENT

The experimental configuration for the proposed multiband sub-THz wireless-over-fiber communication system is shown in Fig. 3. A single light source with a linewidth less than 10 kHz at a wavelength of 1554.98 nm was launched into an OFCG to generate multiple optical tones. The OFCG was based on a dual-drive Mach–Zehnder modulator (MZM) and driven by 15 GHz RF frequency (f_m). This generated phase-correlated
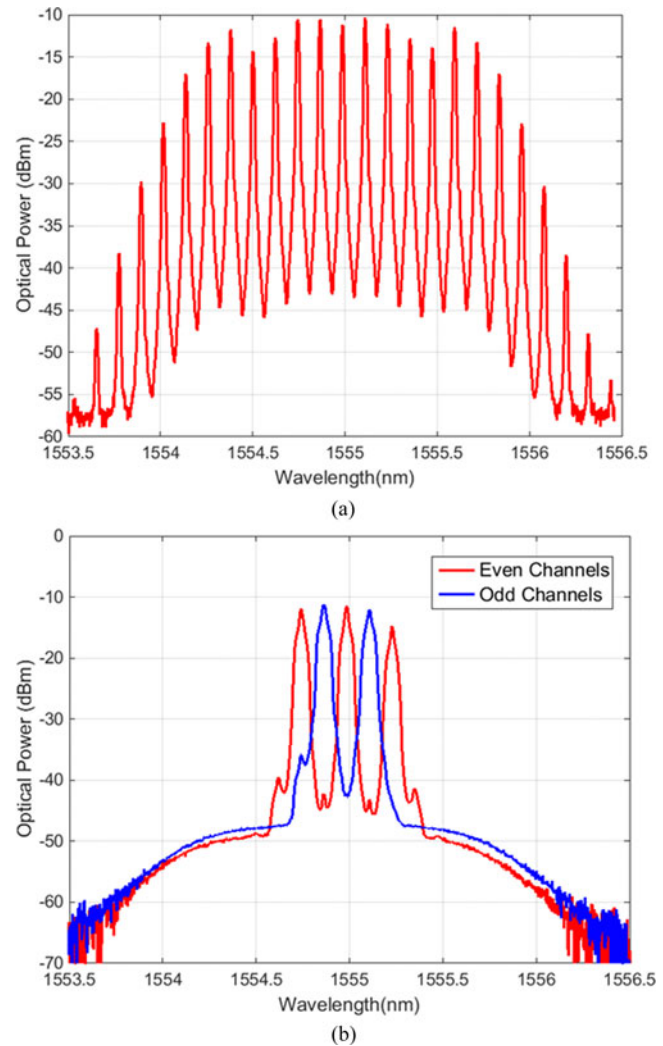
optical subcarriers spaced by the driving RF frequency, as showing in Fig. 4(a). Then, the optical comb was amplified by an erbium-doped fiber amplifier (EDFA) and launched into a WSS to select five optical comb lines and separate them into odd and even subcarriers on two different output ports. Three optical tones (even subcarriers) were injected into one IQ modulator, and the other two optical tones (odd subcarriers) were injected into a second IQ modulator. Both modulators were driven by decorrelated baseband I and Q signals generated from arbitrary waveform generators (AWGs). The AWG outputs (0.5 Vpp) were amplified by baseband amplifiers to drive the IQ modulator with 5.5 Vpp signals, which is enough to drive the optical IQ modulator at the linear region. These baseband amplifiers have 25 dB gain, and 6–11 dB noise figure. The I and Q signals driving the MZM were generated using Matlab offline codes giving 10 Gbaud QPSK filtered by RRC filters with a roll-off factor of 0.01, and with a $2^{11}-1$ pseudo random bit sequence (PRBS) pattern. The output of each IQ modulator was amplified to compensate the insertion loss of the modulator. Then, the modulated optical signals was filtered using a 1 nm optical
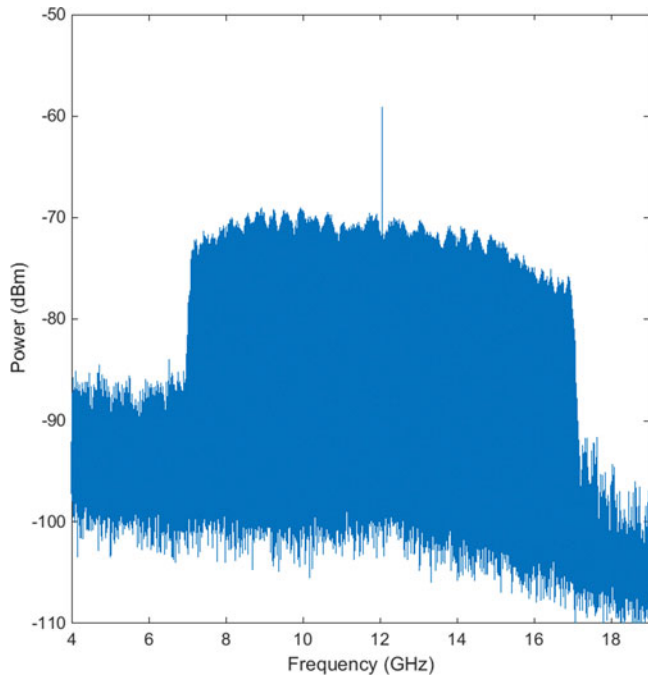
Fig. 5. Electrical spectrum using FFT for the received IF signal.

bandpass filter to remove out-of-band amplified spontaneous emission (ASE). Both optically modulated signals were then combined and transmitted over 10 km of SSMF. Fig. 4(b) shows the modulated optical subcarriers for odd and even channels.

At the RAU, the received optical signal was launched into the optical heterodyne receiver through an optical circulator that separates the uplink from the downlink streams. In the optical heterodyne receiver, the received optical signal was combined first with an optical LO (λ_{LO}) with a wavelength of 1552.95 nm and 100 kHz linewidth. The optical power of the LO signal was controlled to match the total optical power of the modulated channels. Then, the combined signal is amplified and optically filtered using a WSS to select one of the modulated optical sub-carriers and the optical LO signal. The optical LO source beats with the modulated optical subcarrier signal on an unpackaged uni-travelling carrier (UTC) PD with an integrated coplanar waveguide output to generate the sub-THz modulated signal. The output of the PD was coupled to a 20 dBi horn antenna (WR-3.4) using a coplanar mm-wave probe. The modulated THz signal propagated over a wireless channel to a receiving 20 dBi horn antenna. The received THz signal was initially down-converted to a microwave intermediate frequency (IF) by using a sub-harmonic mixer (SHM) operated with an electrical LO. The electrical LO source was obtained using an RF signal generator and a 6X electronic multiplier. The SHM mixes the second harmonic of the electrical LO with the received THz signal. The frequency of the RF signal generator was adjusted to place the IF signal at around 12 GHz, within the frequency band of the analog-to-digital converter in the real time scope (RTS). Then, the received IF signal was amplified and captured by the RTS, whose sampling rate and bandwidth were 80 GSample/s and 36 GHz, respectively. Fig. 5 shows the IF spectrum of the downconverted sub-THz signal obtained by using fast Fourier

transform (FFT) of the data from the RTS. The spectrum has asymmetric shape due to the unflattened response of IF amplifier. The digitized signal was processed offline using the DSP blocks explained previously in [17]. The first DSP step of digital downconversion to the baseband was done using the nominal value of the IF, and then the signal was filtered by RRC of 0.01 roll off factor. The digitized filtered IQ baseband signals were demodulated in subsequent steps of signal resampling, channel equalization based on blind equalization using the constant modulus algorithm, and carrier phase estimation based on the fourth power Viterbi–Viterbi algorithm. After elimination of the $\pi/2$ phase ambiguity, the BER was calculated by directly counting the number of errors in the received bit stream.

The uplink stream was implemented without the wireless channel for simplicity. The uplink data was 10 Gbit/s OOK generated using a pulse pattern generator with a PRBS of $2^{11}-1$ pattern length. The laser used for the optical LO for the optical heterodyne in the downlink steam was also used for the uplink stream. The LO light source (λ_{LO}) was optically modulated with the uplink data using an intensity modulator, and then transmitted through the same SSMF to the central station. There, the upstream optical signal was separated from the downstream signal using an optical circulator, photodetected, amplified and offline demodulated using DSP for measuring its error rate.

IV. RESULTS AND DISCUSSIONS

In this experiment, sub-THz wireless-over-fiber was demonstrated for five bands at sub-THz frequencies of 220, 235, 250, 265, and 280 GHz, as illustrated in the inset to Fig. 3. Each of the bands is modulated with 10 Gbaud (20 Gbit/s) QPSK with Nyquist bandwidth (10 GHz). The performance of this experiment was first determined by measuring the BER for a single carrier transmitted over the fiber, and then with the five optical sub-carriers scheme, as shown in Fig. 6. The BER is plotted on a logarithmic scale against the square of the photocurrent, which is proportional to the received THz power for a fixed wireless link length. In Fig. 6(a), the measured BERs have better performance at 235, 250, and 265 GHz bands. However, the performance is degraded compared to 235 GHz single carrier with 2.6 dB penalty for 220 GHz band and 4.25 dB penalty for 280 GHz band. These degradations are mainly from the UTC-PD frequency response limitation, and the effect of the waveguide response. In the multiband transmission over fiber, the results have been plotted for each filtered band at the RAU, as shown in Fig. 6(b). This shows a similar trend in the variation of the BER for each band, but with larger power penalty compared to the 235 GHz band. The reason for this extra penalty is due to the reduction of optical power per sub-carrier after optical filtering in the case of the multicarrier transmission.

In order to clarify the source of the penalty for each band, we have plotted the average received electrical power and received optical power before PD versus the sub-carrier frequency at BER = 10^{-3} (Fig. 7). This shows that the average received electrical power varies by about 2 dB to obtain the same BER, but shows no particular trend with sub-band frequency. However, more received optical power is required at 280 GHz and
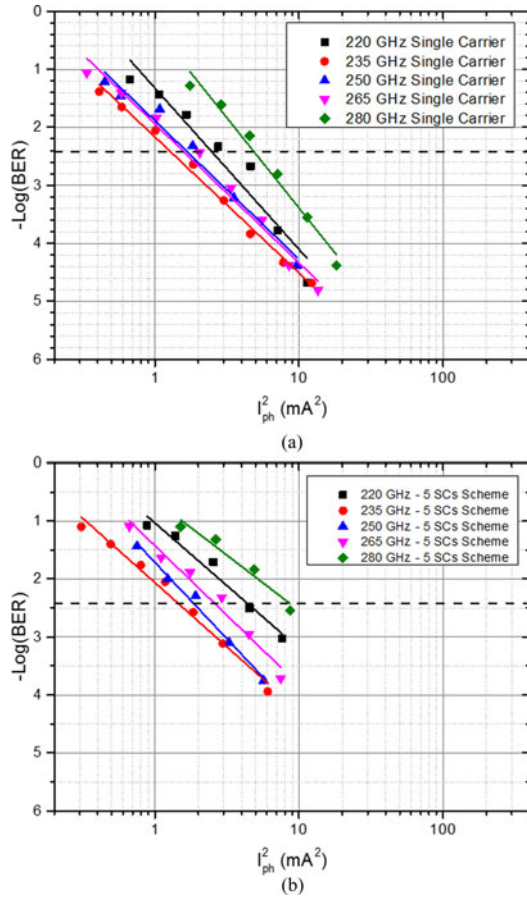
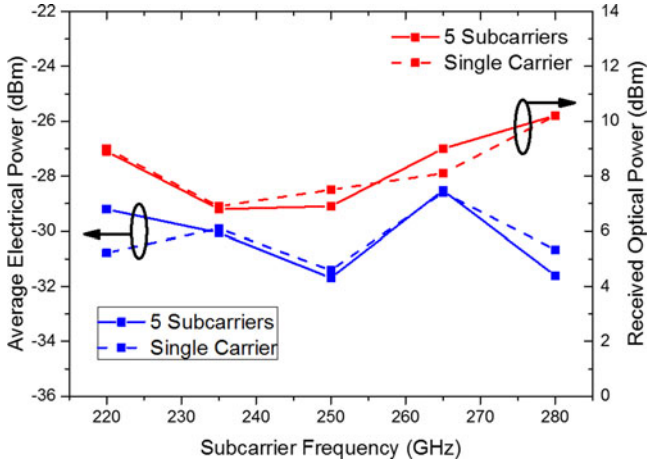Fig. 6.   BER (log scale) versus photocurrent squared for; (a) single band, and (b) multiband scheme.

Fig. 7.   Average received electrical power and received optical power versus subcarrier frequencies.

220 GHz, by 3 dB and 2 dB, respectively, compared to the middle sub-bands, to compensate for lower transmitted power and higher down-conversion loss at these frequencies.

In order to study the impact of the uplink data stream, we investigated the system performance with and without uplink transmission. Fig. 8 shows the BER measured versus the squared photocurrent for a single band at 250 GHz. The penalty when
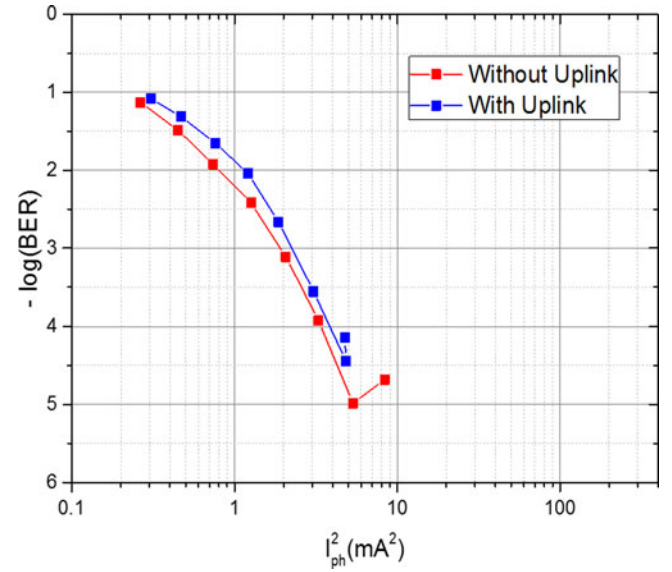

Fig. 8.   BER versus photocurrent squared for downlink at 250 GHz single band with and without uplink transmission.
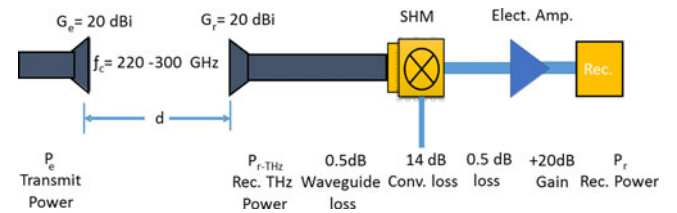

Fig. 9.   Transmission link budget for the downlink at the receiver.

the uplink is in operation is less than 0.74 dB (corresponding to the ratio of the squared photocurrents 1.9 mA^2 and 2.25 mA^2 at BER of 10^{-3} with and without uplink transmission).

V. LINK BUDGET AND FREE SPACE TRANSMISSION

The transmission length used in the experiment was very short (around 2 cm) between the two horn antennas. In order to measure the system performance and to estimate the transmission link length capability, we need to investigate the link power budget of the receiver. Fig. 9 show the coherent detection system comprising an horn antenna WR-3.4 (220 – 330 GHz) with 1 dB waveguide and electrical cable losses, SHM integrated with (6X) multiplier with 14 dB conversion loss, and electrical amplifier with 36 GHz bandwidth and gain of 20 dB. The main noise affecting the system is produced from the combined noise factor of SHM and IF amplifier, which is dominated by the noise factor of the SHM ($\sim$ 30 dB). This has a large impact on the modulated THz signal and degrades the signal-to-noise ratio of the received signal. The amount of noise is increased at higher data rates with larger bandwidth and limits the system transmission links due to the low emitted power from the UTC-PD.

We have measured the frequency response of the wireless link (composed of UTC-PD, waveguides of the horn antennas, SHM, and the electrical amplifier) by measuring the IF power
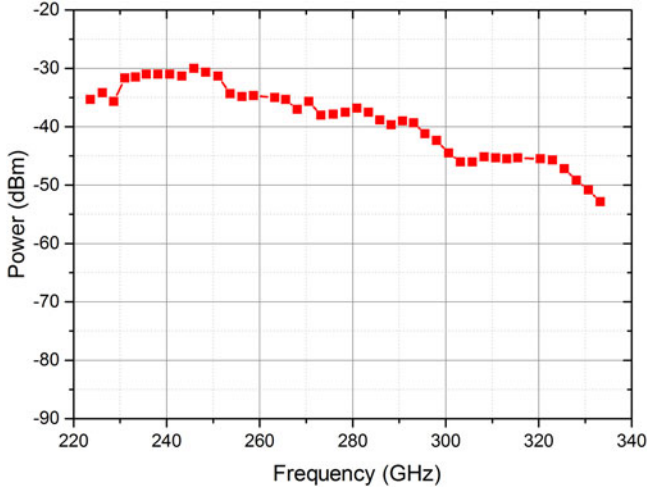
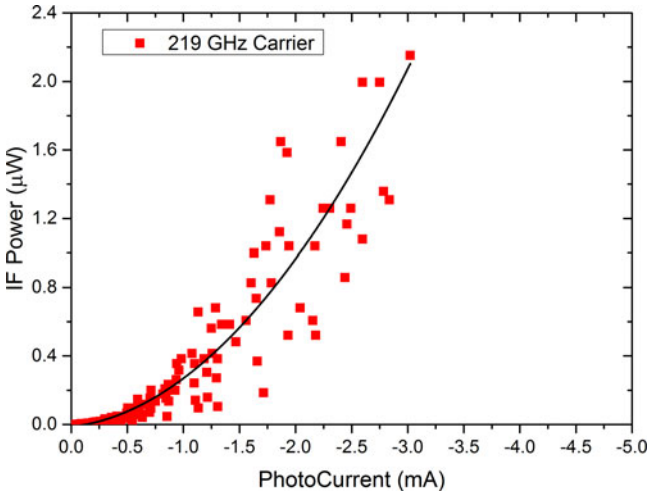Fig. 10. Frequency response measurements for THz receiver.

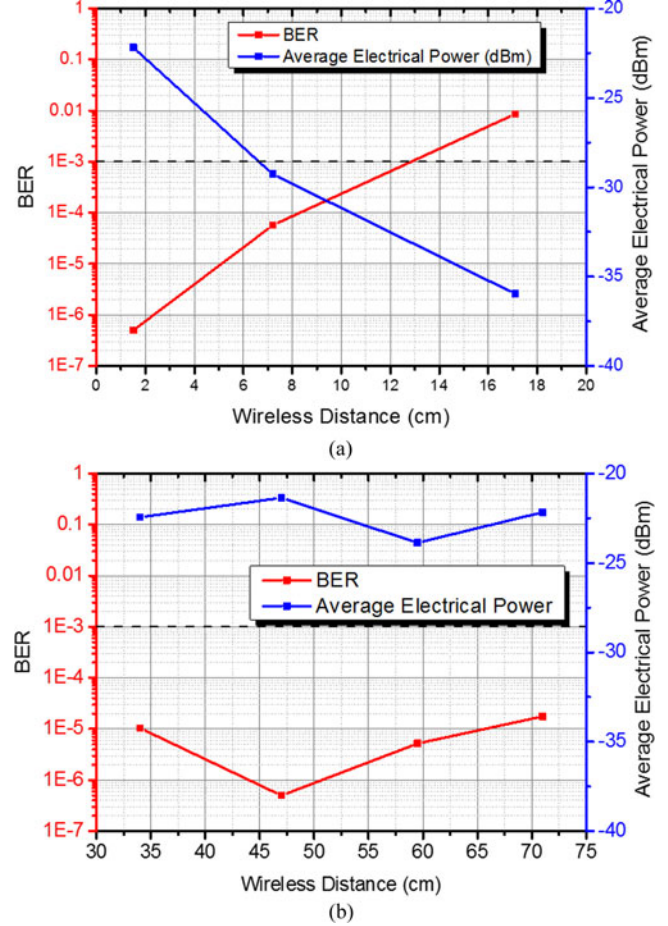Fig 11. IF electrical power versus photocurrent for UTC-PD.

Fig. 12. BER, and average electrical power measurements versus wireless distance for 10 Gbaud QPSK signal with RRC filter (a) without optical lens, and (b) with optical lens.

after down-conversion using a spectrum analyzer for THz carrier frequencies across the band $220 - 330\,\text{GHz}$, generated using an unmodulated optical signal (Fig. 10). The UTC-PD has 0.2 A/W responsivity, and the IF output power measured from the IF amplifier after downconversion is shown in Fig. 11. As can be seen in Fig. 10, the frequency response shows higher power values in the range $230 - 350\,\text{GHz}$ and then its response degrades gradually for frequencies >250 GHz. The edges of the frequency response are affected by the UTC-PD and the waveguide response, and by the SHM's bandwidth (220–330 GHz), therefore there is lower power at 220 GHz. This explains the results shown for BER in the previous section. To estimate the THz received power at the receiver antenna, as illustrated in Fig. 9, we use the following:

$$P_r = P_{r-\text{THz}} - C_L - W_L + G_{\text{ampl}} = P_{r-\text{THz}} + 5\,\text{dB}$$

where P_r is the IF received average power, $P_{r-\text{THz}}$ the THz received power after antenna, C_L the mixer's conversion loss (14 dB), W_L the waveguide and coaxial cable losses (1 dB), and G_{ampl} the amplifier gain (20 dB). From Fig. 10, the electrical

received IF power is -31 dBm at 250 GHz, which means the received THz signal is -36 dBm at the receiver antenna. The FSPL budget at the THz frequency can be also calculated from Friis's equation;

$$\begin{aligned} \text{FSPL (dB)} &= 92.4 - G_e - G_r + 20 \times \log\left(f\,(\text{GHz}) + 20\right. \\ &\quad \left. \times \log\left(d\,(\text{km})\right) + \alpha_{\text{Atm.}}\,(\text{dB/km}) \times d(\text{km})\right) \end{aligned}$$

where f is the THz frequency in GHz, d is the transmission length in km, G_e and G_r are emitter and receiver antenna gains (20 dBi), respectively and $\alpha_{\text{Atm.}}$ is the specific attenuation of the transmission media (2–5 dB/km). The loss for the free space link for short distance (2 cm) is found to be 6.4 dB. Then, the transmitted power can be estimated to be -29.6 dBm. To indicate the low power required for data transmission, the BER and average received power were measured versus wireless link distance for 10 Gbaud QPSK at 200 GHz carrier frequency with 0.01 RRC filter (Fig. 12). At the limit of FEC (BER < 10^{-3}), the wireless distance was increased to 13 cm for an average received IF power of -35 dBm. The wireless link length was further extended by using optical lenses (made of polymethylpentene material) with 50 mm diameter between the two horn antennas to collimate the beam, as shown in Fig. 13. The link length was increased to over 70 cm, while maintaining
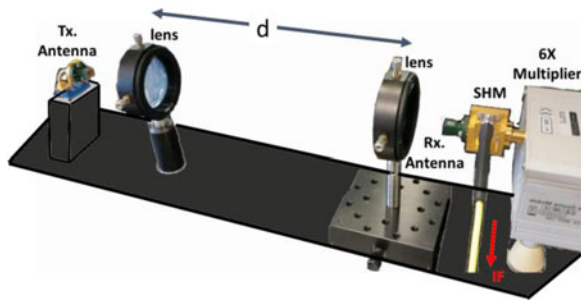
Fig. 13. Photograph of the wireless configuration using two optical lenses.

a BER well below the FEC limit. This suggests the link length could be considerably extended with this lens configuration. However, fluctuations in BER and power were observed due to alignment errors, and these would be expected to become more significant as the transmission distance is further increased. These results indicate that transmission using higher UTC-PD output power combined with optical lenses will be required for realistic short-range wireless coverage. As has been shown, the transmission distance is still limited due to the low output of UTC-PD. An alternative solution would be to use new advanced active array antennas to increase power and to enable mobile device tracking. The implementation of the THz amplifier is already available and feasible to produce around 10 dBm output power [20], [21].

VI. CONCLUSION

We have successfully demonstrated a photonically generated multiband sub-THz bi-directional wireless-over-fiber communication system, with downlink at up to 100 Gbit/s in total (20 Gbit/s per channel at 1.33 bit/s/Hz spectral efficiency), with 10 Gbit/s OOK on the uplink optical stream. This system approach presents five bands at sub-THz across the whole spectrum from 220–280 GHz, with each band modulated with spectrally efficient modulation at 10 Gbaud QPSK with Nyquist bandwidth using RRC filter with 0.01 roll off factor. The system performance was evaluated for single- and multi-band schemes by measuring the BER using offline DSP at the receiver. The system performance was found to be dependent on the UTC-PD and waveguide bandwidths. The receiver link power budget and receiver losses were examined in terms of the received electrical power and BER. The wireless distance can be further expanded to more than 1 m with BER still less than FEC limit, limited only by the need to align the transmitter and receiver antennas with high accuracy. This approach offers a solution for the expected future increased demand in wireless communication, giving more bandwidth, and allowing frequency reuse capability. In addition, this system offers an easy and power efficient system for down/uplink distribution.

REFERENCES

[1] Cisco and/or its Affiliates, "Cisco Visual Networking Index: Global Mobile Data Traffic Forecast Update, 2014–2019," pp. 1–42, 2015.

[2] "Internet of Things market to reach $1.7 trillion by 2020: IDC - MarketWatch." [Online]. Available: http://www.marketwatch.com/story/internet-of-things-market-to-reach-17-trillion-by-2020-idc-2015-06-02-8103241. Accessed: 2015.

[3] J. G. Andrews, S. Buzzi, W. Choi, S. V. Hanly, A. Lozano, A. C. K. Soong, and J. C. Zhang, "What will 5G be?" *IEEE J. Sel. Areas Commun.*, vol. 32, no. 6, pp. 1065–1082, Jun. 2014.

[4] A. Seeds, H. Shams, M. Fice, K. Balakier, L. Ponnampalam, and C. Renaud, "Prospects for millimetre-wave-over-fiber and THz-over-fiber systems," *Proc. SPIE*, vol. 9387, 2015, Art. no. 938702.

[5] Radiocommunication Sector of International Telecommunication Union, "P.676-10: Attenuation by atmospheric gases," in *P Series, Radiowave Propagation*, vol. 10, pp. 1–21, 2013.

[6] A. Hirata *et al.*, "120-GHz-band wireless link technologies for outdoor 10-Gbit/s data transmission," *IEEE Trans. Microw. Theory Techn.*, vol. 60, no. 3, pp. 881–895, Mar. 2012.

[7] A. Kanno, K. Inagaki, I. Morohashi, T. Sakamoto, T. Kuri, I. Hosako, T. Kawanishi, Y. Yoshida, and K. Kitayama, "20-Gbit/s QPSK W-band (75-110GHz) wireless link in free space using radio-over-fiber technique," *IEICE Electron. Express*, vol. 8, no. 8, pp. 612–617, 2011.

[8] A. Kanno, K. Inagaki, I. Morohashi, T. Sakamoto, T. Kuri, I. Hosako, T. Kawanishi, Y. Yoshida, and K. Kitayama, "40 Gbit/s W-band (75–110 GHz) 16-QAM radio-over-fiber signal generation and its wireless transmission," *Opt. Express*, vol. 19, no. 26, pp. B56–63, 2011.

[9] X. Pang, A. Caballero, A. Dogadaev, V. Arlunno, R. Borkowski, J. S. Pedersen, L. Deng, F. Karinou, F. Roubeau, D. Zibar, X. Yu, and I. T. Monroy, "100 Gbit/s hybrid optical fiber-wireless link in the W-band (75–110 GHz)," *Opt. Express*, vol. 19, no. 25, pp. 24944–24949, Dec. 2011.

[10] X. Li *et al.*, "Fiber-wireless-fiber link for 128-Gbit/s PDM-QPSK signal transmission at W-band," *IEEE Photon. Technol. Lett.*, vol. 26, no. 19, pp. 1948–1951, Oct. 2014.

[11] M. Beltran *et al.*, "Single-and multiband OFDM photonic wireless links in the 75–110 GHz band employing optical combs," *IEEE Photon. J.*, vol. 4, no. 5, pp. 2027–2036, Oct. 2012.

[12] J. Zhang, J. Yu, C. Nan, D. Ze, L. Xinying, and G. K. Chang, "Multichannel 120-Gbit/s data transmission over 2×2 MIMO fiber-wireless link at W-band," *IEEE Photon. Technol. Lett.*, vol. 25, no. 8, pp. 780–783, Apr. 2013.

[13] S. Koenig, D. Lopez-Diaz, J. Antes, F. Boes, R. Henneberger, A. Leuther, A. Tessmann, R. Schmogrow, D. Hillerkuss, R. Palmer, T. Zwick, C. Koos, W. Freude, O. Ambacher, J. Leuthold, and I. Kallfass, "Wireless sub-THz communication system with high data rate," *Nature Photon.*, vol. 7, no. 12, pp. 977–981, Oct. 2013.

[14] T. Nagatsuma, S. Horiguchi, Y. Minamikata, Y. Yoshimizu, S. Hisatake, S. Kuwano, N. Yoshimoto, J. Terada, and H. Takahashi, "Terahertz wireless communications based on photonics technologies," *Opt. Express*, vol. 21, no. 20, pp. 477–487, 2013.

[15] H. Ito, S. Kodama, and T. Ishibashi, "InP/InGaAs uni-travelling-carrier photodiode with 310 GHz bandwidth," *Electron. Lett.*, vol. 36, no. 21, pp. 1809–1810, 2000.

[16] G. Ducournau *et al.*, "Ultrawide bandwidth single channel 0.4 THz wireless link combining broadband quasi-optic photomixer and coherent detection," *IEEE Trans. Terahertz Sci. Technol.*, vol. 4, no. 3, pp. 328–337, May 2014.

[17] H. Shams, M. J. Fice, K. Balakier, C. C. Renaud, F. van Dijk, and A. J. Seeds, "Photonic generation for multichannel THz wireless communication," *Opt. Express*, vol. 22, no. 19, pp. 23465–23472, Sep. 2014.

[18] H. Shams, M. J. Fice, K. Balakier, C. C. Renaud, A. J. Seeds, and F. Van Dijk, "Multichannel 200 GHz 40 Gbit/s wireless communication system using photonic signal generation," in *Proc. Int. Top. Meet. Microw. Photon./9th Asia-Pacific Microw. Photon. Conf.*, Oct. 20–23, 2014, pp. 4–7.

[19] H. Shams *et al.*, "100 Gbit/s multicarrier THz wireless transmission system with high frequency stability based on a gain-switched laser comb source," *IEEE Photon. J.*, vol. 7, no. 3, pp. 1–11, Jun. 2015.

[20] A. Tessmann, A. Leuther, V. Hurm, H. Massler, M. Zink, M. Kuri, M. Riessle, R. Lösch, M. Schlechtweg, and O. Ambacher, "A 300 GHz mHEMT amplifier module," in *Proc. IEEE Int. Conf. Indium Phosphide Related Mater.*, 2009, pp. 196–199.

[21] J. C. Tucek, M. A. Basten, D. A. Gallagher, and K. E. Kreischer, "220 GHz power amplifier development at Northrop Grumman," in *Proc. IEEE 13th Int. Conf. Vacuum Electron. Conf.*, 2012, pp. 553–554.

Haymen Shams received the B.Sc. and M.Sc. degrees in electrical and electronic engineering from Alexandria University, Alexandria, Egypt, in 1999 and 2006, respectively and the Ph.D. degree in electrical and electronic engineering from Dublin City University, Dublin, Ireland, in 2011. His Ph.D. dissertation addresses the optical technologies for generation and distribution of millimeter waves and ultra-wideband RF signals in radio-over-fiber systems. In 2011, he joined the photonics group at Tyndall national institute, University College Cork, Ireland, for two years. He is currently a Research Associate in the Photonic Groups, Department of Electrical and Electronic Engineering, University College London. His research areas of interest include RF-over-fiber for wireless communication including ultra wideband and millimeter wave signals, different optical modulation level formats (such as QPSK, QAM, and CO-OFDM), digital coherent receivers, digital signal processing, and optical comb generation.

Dr. Shams is a Member of Institute of Electronic and Electrical Engineering and European Physical Society.

Martyn J. Fice (S'86–M'87) received the B.A. degree in electrical science and the Ph.D. degree in microelectronics from the University of Cambridge, Cambridge, U.K., in 1984 and 1989, respectively.

In 1989, he joined STC Technology Laboratories, Harlow, U.K. (later acquired by Nortel), where he was engaged for several years in the design and development of InP-based semiconductor lasers for undersea optical systems and other applications. Subsequent work at Nortel involved research into various aspects of optical communications systems and networks, including wavelength-division multiplexing, all-optical wavelength conversion, optical regeneration, and optical packet switching. In 2005, he joined the Photonics Group, Department of Electronic and Electrical Engineering, University College London, London, U.K., as a Senior Research Fellow. He is currently a Lecturer in the same department, with research interests in millimeter and THz wave generation and detection, optical phase locking, coherent optical detection, optical transmission systems, and photonic integration.

Dr. Fice is a Member of the Institution of Engineering and Technology and a Chartered Engineer.

Luis Gonzalez-Guerrero received the B.Sc. degree in materials engineering from the Technical University of Madrid, Madrid, Spain, in 2013 and the M.Sc. degree in photonics and optoelectronics devices from the University of St Andrews and Heriot-Watt University, U.K., in 2014. His master thesis was about the design, analysis, and optimization of diffractive elements for distance ranging applications. He is currently working toward the Ph.D. degree in electronic engineering at University College London in collaboration with the National Physical Laboratory. His research interests include THz wireless communications, especially on the characterization and application of photonic integrated chips in THz links and on the characterization of coherent and non-coherent systems.

Cyril C. Renaud received the degree of engineering from the Ecole Supérieure d'Optique, Orsay, France, and the Diplôme d'Etudes Approfondies in optics and photonics from the University Paris XI, Orsay, France, in 1996. He spent one year as a Project Engineer with Sfim-ODS, working on the development of microchips lasers. He then worked within Optoelectronics Research Centre, University of Southampton, Southampton, U.K., on diode pumped high-power ytterbium-doped fiber-lasers, with particular interest on Q-switched system and 980-nm generation. This work led to the award of a Ph.D. degree in 2001. He is currently a Senior Lecturer and Site Director of a doctoral training center at University College London, U.K., where he is working on optoelectronic devices and systems. His current research interests include works on uncooled WDM sources, agile tuneable laser diode and monolithic optical frequency comb generator using Quantum Confined Stark Effect, high frequency photodetectors (UTC, travelling wave) and optical frequency generation systems in the optical and millimeter wave domains (DWDM, THz).

Frédéric van Dijk works at III-V Lab, a joint Laboratory of "Alcatel Lucent Bell Labs," "Thales Research & Technology," and "CEA-LETI." He is leading the "photonic device for optronics" team involved in design, fabrication and characterization of optoelectronic devices for microwave and sensing applications. He is in particular studying directly modulated DFB lasers for low loss high dynamic range analog links, mode-locked lasers for telemetry and high speed data sampling, dual wavelength lasers, and photonic integrated circuits on InP for microwave to terahertz wave generation.

Alwyn J. Seeds (M'81–SM'92–F'97) received the B.Sc., Ph.D., and D.Sc. degrees from the University of London, London, U.K. From 1980 to 1983, he was a Staff Member at Lincoln Laboratory, Massachusetts Institute of Technology, where he worked on GaAs monolithic millimeter-wave integrated circuits for use in phased-array radar. Following three years as Lecturer in telecommunications at Queen Mary College, University of London he moved to University College London in 1986, where he is currently a Professor of opto-electronics and the Head of the Department of Electronic and Electrical Engineering. He has published more than 350 papers on microwave and opto-electronic devices and their systems applications. His current research interests include semiconductor opto-electronic devices, wireless and optical communication systems.

Professor Seeds is a Fellow of the Royal Academy of Engineering (U.K.). He has been a Member of the Board of Governors and Vice-President for Technical Affairs of the IEEE Photonics Society (USA). He has served on the program committees for many international conferences. He is a co-founder of Zinwave, a manufacturer of wireless over fiber systems. He received the Gabor Medal and Prize of the Institute of Physics in 2012.